

Report Number 10/44

Mud peeling and horizontal crack formation in drying clays

by

Robert W. Style, Stephen S. L. Peppin and Alan C. F. Cocks



Oxford Centre for Collaborative Applied Mathematics
Mathematical Institute
24 - 29 St Giles'
Oxford
OX1 3LB
England

Mud peeling and horizontal crack formation in drying clays.

Robert W. Style, Stephen S. L. Peppin and Alan C. F. Cocks

August 5, 2010

Abstract

Mud peeling is a common phenomenon whereby horizontal cracks propagate parallel to the surface of a drying clay. Differential stresses then cause the layer of clay above the crack to curl up to form a mud peel. By treating the clay as a poroelastic solid, we analyse the peeling phenomenon and show that it is caused by the gradient in tensile stress at the surface of the clay, analogously to the spalling of thermoelastic materials. For a constant water evaporation rate at the clay surface we derive equations for the depth of peeling and the time of peeling as functions of the evaporation rate. Our model predicts a simple relationship between the radius of curvature of a mud peel and the depth of peeling. The model predictions are in agreement with the available experimental data available.

1 Introduction

Mud cracking is a process commonly found in hot, dry climates in regions where a clayey soil has been recently saturated with water such as intertidal regions or deserts after a rainfall. There are two main types of fractures that occur during drying. The first type propagate perpendicular to the clay surface causing the soil to fracture into polygonal sections. These shrinkage cracks and the process behind the associated polygonal pattern formation have been well-studied and are the subject of active research [1, 2].

The second type of fracture that occurs in concert with the formation of shrinkage cracks is the formation of ‘mud curls’ or mud peeling. In this case a ‘peeling’ crack propagates parallel to the surface of the clay. Depending on the thickness of the peeled layer, the peel can then roll up to leave a characteristic mud curl as shown in figure 1. It can be seen that this type of fracture can lead to interestingly sculpted clay shapes. However beyond a



Figure 1: Mud curls and desiccation polygons formed by the rapid drying of clay in Death Valley, CA. The largest polygons are approximately 30cm in length while mud peels are around 2mm in thickness (photograph courtesy of Don Gale).

desire to understand such pattern formations it is also important to understand mud curl formation for practical reasons. The fracture process breaks up the soil and impacts the moisture retention during further evaporation, soil permeability, nutrient content and distribution in the soil, and the characteristics of the topsoil [3, 4]. All of these factors are important for plant growth, and the effects on permeability are also of interest in clay liners for reservoirs and hazardous waste storage containers where leakoff is highly undesirable [4]. In addition mud curls can be brittle and delicate objects which means that they are susceptible to break up into smaller particles which may be blown away in strong winds.

Previous studies of mud curl formation have attributed their formation to delamination of a clay curl from an underlying substrate consisting of a material of differing composition (e.g. [5]). However figure 1 clearly shows evidence of secondary curls forming beneath the initial curls on the surface of the drying clay. These secondary curls have a roughly similar thickness to the primary curls ($\sim 1\text{-}2\text{mm}$ in comparison to a polygon width of $\sim 30\text{cm}$).

As it is unlikely that there exist two layers of clay at the surface of the soil, each of a thickness of around 1mm, this suggests that there is an additional mechanism that can drive the formation of peeling cracks.

In this paper we demonstrate that peeling cracks can be formed by the rapid drying of a saturated clay after shrinkage cracks have developed perpendicular to the drying front. We treat the clay as a poroelastic solid and show that mud curl formation is the poroelastic analogue of spalling due to the imposition of temperature gradients in a thermoelastic solid (e.g. [6]). Cracking is driven by stress gradients in the clay induced by pore pressure changes associated with the directional drying at the soil surface. As we shall see the depth of peeling from the polygon surface is predominantly controlled by the evaporation rate and the permeability of the clay.

2 Clay desiccation during constant surface evaporation

In this section we introduce the equations of poroelasticity that we use to describe a drying clay. Drying from a surface occurs in two stages. In the first stage the clay remains saturated with liquid as the constituent particles consolidate together due to the reducing liquid pressure in the pores of the clay. In this stage tensile stresses form that can give rise to primary, craquelure-type cracking [1] and, as we shall show, peeling cracks. After sufficient drying has occurred a desaturation front will appear as air enters the pores of the clay. A second type of cracking, known as columnar jointing, can occur associated with this drying front (e.g. [7]) however in this paper we shall only consider primary crack formation and treat the clay as always being saturated. This assumption can be justified from experimental evidence showing that stresses increase as a solid dries until the drying front enters the body of the solid. At this point the low pore pressure that causes the existence of tensile stress disappear and these stresses start to relax (e.g. [8, 9]). Therefore the greatest tensile stresses available to cause primary fracture are present before desaturation occurs and crack formation will occur while the material is fully saturated.

Clay is a complicated material that has varying nonlinear properties depending strongly on clay particle concentration. However it has been shown that muds of high clay concentration, such as considered here, have a substantial linear elastic response [10]. Indeed the assumption that clay behaves elastically until it reaches its yield locus forms the basis of the Cam-clay theory of soil mechanics [11]. Therefore in this paper we shall take the

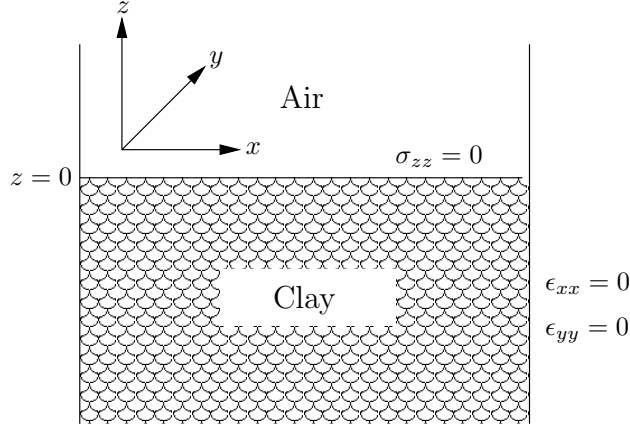


Figure 2: Schematic diagram for the drying of clay. The column of clay is held under uniaxial strain conditions and the vertical stress is zero.

clay as having been lightly over-consolidated so that we may assume that it is linearly poroelastic in behaviour. This is a common assumption in the treatment of soil fracture (e.g. [12]) and has the added benefit of allowing us to use linear elastic fracture mechanics to investigate the fracture mechanism involved in mud peeling, thereby simplifying the physics involved and giving us a good understanding of the physical process underlying the phenomenon.

The linear poroelastic constitutive relation is given by

$$\sigma_{ij} = 2G\epsilon_{ij} + 2G\frac{\nu}{1-2\nu}\epsilon_{kk}\delta_{ij} - \alpha(p-p_0)\delta_{ij} \quad (1)$$

[13] where we have used standard notation so that σ_{ij} is the stress on the body, ϵ_{ij} is the strain, G is shear modulus, ν is Poisson's ratio, α is the Biot-Willis coefficient, p is the pore pressure, p_0 is the initial pressure at which there is no stress in an unstrained, isotropic body and δ_{ij} is the Kronecker delta. As clay particles are generally considered to be incompressible we can set $\alpha = 1$ [13]. In order to determine the tensile stresses in the body of the clay we require the pore pressure distribution in the clay. We consider initially the unfractured situation shown in figure 2 where the clay is assumed to be of large vertical extent so that no shrinkage can occur in the x or y directions and the horizontal strains ϵ_{xx} and ϵ_{yy} are zero (uniaxial strain conditions). In addition the top of the clay is open to the air at atmospheric pressure p_a so neglecting gravity we can assume the vertical stress $\sigma_{zz} = -p_a$ throughout the height of the column.

By use of Darcy's Law for flow through a porous medium and a second constitutive relation for the increment of fluid content, Wang [13] shows that under uniaxial strain and constant vertical stress the pore pressure in the clay satisfies the equation

$$\frac{\partial p}{\partial t} = c \frac{\partial^2 p}{\partial z^2}, \quad (2)$$

where c is the hydraulic diffusivity of the clay. c depends linearly upon permeability and therefore depends strongly on the type of clay. For example, in low permeability clays such as bentonite $c \approx 5 \times 10^{-10} \text{m s}^{-1}$ while in more permeable clays such as kaolinite, $c \approx 5 \times 10^{-7} \text{m s}^{-1}$ [14].

We shall make the simplifying assumption that there is a steady rate of evaporation E from the clay-air interface where E is quantified as the volume flux of water away from the surface per unit time per unit surface area. Then Darcy's law at the clay-air interface gives

$$E = -\frac{k}{\mu} \frac{\partial p}{\partial z} \Big|_{z=0} \quad (3)$$

where k is the permeability of the clay, μ is the dynamic viscosity of the clay and we have defined our co-ordinate system with $z = 0$ corresponding to the clay-air interface.

Our assumption of constant evaporation rate warrants some justification. We envisage two distinct scenarios in which suitable conditions for cracking may occur. Firstly, we consider the case of an intertidal region when the tide recedes leaving wet clay exposed to warm dry conditions. Secondly, we consider the case of hot, dry desert-like conditions where the exposed soil comprises a clayey material, after an event such as a rain storm. As the tide recedes or as the rain gives way to desert sun, the clay will initially be waterlogged but will rapidly drain to give a uniform, saturated poroelastic solid under relatively constant dry atmospheric conditions. In these conditions the evaporation is well-approximated by a constant up to the point at which air invades the pores of the clay and so we can assume a steady evaporation rate at the clay-air interface. We note this approximation has been well verified experimentally and is a commonly used approximation in the drying literature (e.g. [15, 9]).

The clay is initially uniform after draining from a waterlogged state so we treat the process as beginning from a state of uniform pressure p_0 . The solution to equation (2) based on a constant initial condition with a constant

pressure gradient at the surface is

$$p(z, t) = p_0 - 2 \frac{E\mu}{k} \left[\left(\frac{ct}{\pi} \right)^{1/2} e^{-z^2/4ct} + \frac{z}{2} \operatorname{erfc} \left(\frac{-z}{2\sqrt{ct}} \right) \right] \quad (4)$$

(e.g. [16]) which gives the evolving pore pressure distribution as a function of z and t . Here erfc is the complementary error function [17].

In order to find the stress distribution in the clay we use equation (1) under uniaxial strain and constant vertical stress to find that the horizontal stresses are given by

$$\sigma_{xx} = \sigma_{yy} = \frac{1 - 2\nu}{1 - \nu} \alpha(p_0 - p), \quad (5)$$

where we have made the approximation that the atmospheric pressure, p_a is zero as it is small relative to capillary pressures that arise during drying and so $\sigma_{zz} = 0$. The combination of equations (4) and (5) then yields the horizontal stress distribution in the drying clay. In the next section we shall demonstrate how the increasing gradient in tensile stress at the clay surface leads to mud peel formation.

3 Spall crack formation

We treat the mud peeling process as being the opening of a delamination crack shown schematically in figure 3(a). During drying, tensile stresses arise at the surface of the clay which can lead to shrinkage cracks perpendicular to the clay surface. Once a shrinkage crack has formed delamination cracks can appear that travel sideways from the shrinkage crack (not necessarily parallel to the drying surface). These delamination cracks are driven by the relaxation of stresses in the peel reducing the stored strain energy in the system as the cracks propagate [6].

Delamination cracks should propagate quickly once initiated and so during the crack growth there will be little movement of water between the pores of the solid. Under these ‘undrained’ conditions Rice and Cleary [18] have shown that a linearly poroelastic solid behaves as a linearly elastic solid with the same shear modulus G , but with an undrained Poisson’s ratio ν_u that depends on ν and Skempton’s coefficient [13]. This means that we can treat the crack as appearing in a linearly elastic body with an applied stress distribution given by combining equations (4) and (5) and we can make use of linear elastic fracture mechanics, in particular previous work on delamination cracking in order to analyse crack growth.

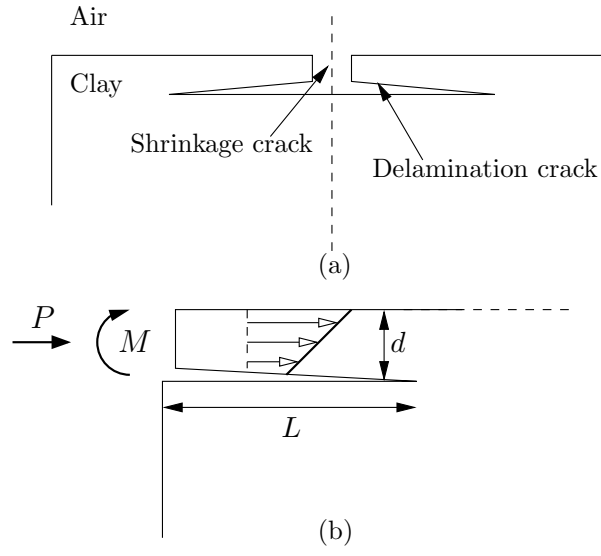


Figure 3: Schematic diagram for crack formation in a drying clay. (a) Shrinkage and delamination cracks. (b) Close-up of a delamination crack showing the stress distribution in the mud peel and defining quantities used in the text.

Hutchinson and Suo [6] show that the problem of a linear elastic solid under a tensile stress distribution can be reduced by linear superposition to the problem shown in figure 3(b). A thin peel cracks away from the surface of the drying clay with the stress distribution in the peel given by the stress distribution in the uncracked body. We consider the steady-state opening of the crack so that the peel thickness d is much smaller than the length of the crack L , then using Saint-Venant's principle we can replace the stress distribution on the peel with a force per unit depth (in the y direction) P and a moment per unit depth M where

$$P = \int_{-d}^0 \sigma_{xx} dz \quad (6)$$

and

$$M = \int_{-d}^0 \left(z + \frac{d}{2} \right) \sigma_{xx} dz \quad (7)$$

[6].

Thouless et al. [19] have shown that for a semi-infinite solid as considered here, the mode I and mode II stress intensity factors K_I and K_{II} at the tip of the delamination crack are related to P and M by

$$K_I = \frac{P \cos \omega}{\sqrt{2d}} + \frac{\sqrt{6}M \sin \omega}{d^{3/2}} \quad (8)$$

and

$$K_{II} = \frac{P \sin \omega}{\sqrt{2d}} - \frac{\sqrt{6}M \cos \omega}{d^{3/2}}, \quad (9)$$

where $\omega = 52.07^\circ$.

If the clay is a homogeneous (unstratified) solid the delamination crack can only propagate in a straight line parallel to the surface if the mode II stress intensity factor is zero so that the crack opening is purely mode I [6]. In addition for the crack to propagate $K_I \geq K_{Ic}$, with K_{Ic} being the mode I fracture toughness of the clay which has units of $\text{Pa m}^{1/2}$. By application of these two conditions we can determine the depth of steady-state cracking and the amount of time taken after the initiation of drying for cracking to appear.

Inserting the expressions for the tensile stress in the clay (4,5) into equations (6,7) we find that

$$P = \sigma_0 \frac{d^2}{\xi^2} \int_0^\xi \left(\frac{e^{-u^2}}{\sqrt{\pi}} - u \cdot \text{erfc} u \right) du \quad (10)$$

and

$$M = \sigma_0 \frac{d^3}{\xi^3} \int_0^\xi \left(-u + \frac{\xi}{2} \right) \left(\frac{e^{-u^2}}{\sqrt{\pi}} - u \cdot \text{erfc}u \right) du \quad (11)$$

where $\sigma_0 \equiv (1 - 2\nu)\alpha E\mu/(1 - \nu)k$, $u = -z/2\sqrt{ct}$ is a similarity variable and $\xi = d/2\sqrt{ct}$ is the nondimensional thickness of the peel.

Inserting these expressions into equation (9) with $K_{II} = 0$ we obtain an integral equation for ξ

$$\int_0^\xi \left(\frac{ue^{-u^2}}{\sqrt{\pi}} - u^2 \cdot \text{erfc}u \right) du = \xi \left[\frac{1}{2} - \frac{\tan \omega}{\sqrt{12}} \right] \int_0^\xi \left(\frac{e^{-u^2}}{\sqrt{\pi}} - u \cdot \text{erfc}u \right) du \quad (12)$$

which can be solved numerically to give $\xi = 2.9026$. Using this result in equations (10,11) and requiring that $K_I = K_{Ic}$ in equation (8) gives $d = 9.5032(K_{Ic}/\sigma_0)^{2/3}$ or expanding σ_0 ,

$$d = 9.5032 \left(\frac{(1 - \nu)K_{Ic}k}{(1 - 2\nu)\alpha E\mu} \right)^{2/3}, \quad (13)$$

while the definition of ξ gives the time at which cracking occurs,

$$t = \frac{d^2}{33.70c}. \quad (14)$$

4 Results and discussion

In order for the mode I solution obtained above to be expressed during drying we must show that the solution is stable to perturbations. Figure 4 shows the mode mixity $\psi = \tan^{-1}(K_{II}/K_I)$ of a crack growing at a depth z . When the mode mixity is non-zero it approximates the angle to the horizontal at which a crack will propagate (e.g. [6]). Thus when $\psi > 0$ the crack will propagate downwards, while when $\psi < 0$ the crack propagates upwards towards the clay-air interface (e.g. [6]). From figure 4 we can therefore see that cracks forming away from the steady state cracking depth (the dashed line) will converge back towards it. This means that the mode I crack is stable and therefore physically realisable.

We can use the results calculated above to estimate the thicknesses of mud peels arising in drying conditions. Typical parameter values for the three main groups of clays (bentonite, illite and kaolinite) are given in table 1 along with references for the source of these values. In addition we take

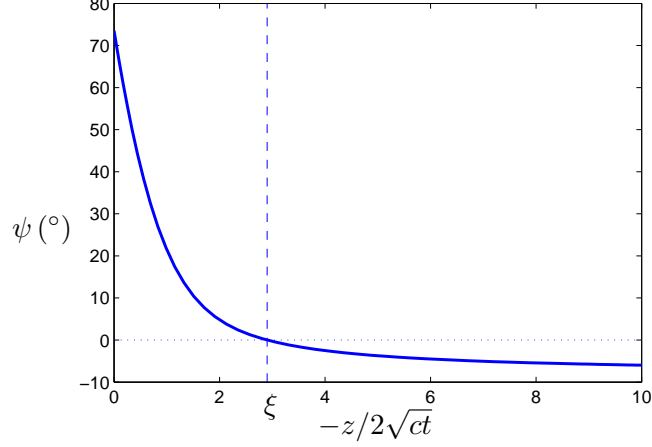


Figure 4: Mode mixity of a crack forming at a depth z , plotted in terms of the dimensionless length $u = -z/\sqrt{ct}$. Continuous curve: mode mixity. Dotted line: $\psi = 0$ which corresponds to $K_{II} = 0$. Dashed line: steady-state cracking depth.

the dynamic viscosity of water as $10^{-3} \text{ kg m}^{-1} \text{ s}^{-1}$. Evaporation rates from saturated soils in warm climates are around 0.7 mm hr^{-1} which corresponds to $E = 1.9 \times 10^{-7} \text{ m s}^{-1}$ [20]. Therefore we estimate evaporation rates in typical drying conditions to be $\sim 10 \times 10^{-7} \text{ m s}^{-1}$. Evaporation rates from wet soils in desert conditions can reach 22.9 mm day^{-1} [21], so assuming that the majority of evaporation occurs during 12 hours of daylight, we estimate a peak desert daytime evaporation rate of approximately $6 \times 10^{-7} \text{ m s}^{-1}$.

Figure 5 shows the predicted peel thickness as a function of evaporation rate for each type of clay. This shows that a low permeability clay such as bentonite will fracture at a depth of 0.4mm or more. Illite, a more permeable clay, will fracture at a depth of 3mm or more. Kaolinite, the most porous of the three clays, will fracture at a depth of approximately 1cm or more.

Unfortunately there is little quantitative experimental evidence to test against our theory. However Allen studied mud peeling in the Severn estuary where the clay has been shown to be predominantly illite [5, 28]. In his observations it was found that peels had typical thicknesses of $O(2 \text{ cm})$ while we have estimated the evaporation rate above to be $O(10^{-7}) \text{ m s}^{-1}$. This point is shown in figure 5 to be in line with predicted peel thicknesses for illite. In addition Konrad and Ayad[27] observed horizontal spalling cracks

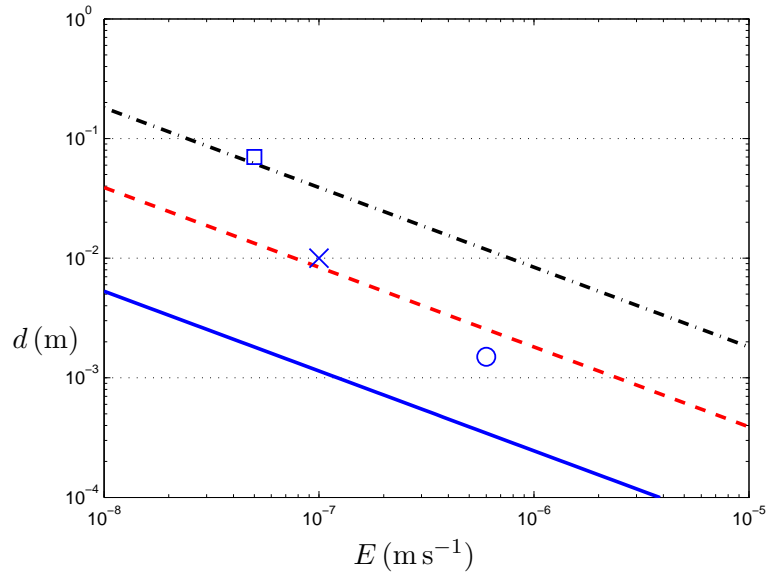


Figure 5: Peel thickness as a function of evaporation rate calculated for three types of clay. Continuous line: bentonite. Dashed line: illite. Dash-dotted line: kaolinite. \square Experimental data of Konrad and Ayad [27]. \times Observations of Allen [5]. \circ Observations of peeling in Death Valley, CA.

Table 1: Data specific to types of clay. Poisson’s ratios are taken from Morris et al. [12]. Permeabilities are typical figures estimated from Robinson & Allam [14], Pane & Schiffman [22], and Peppin et al. [23]

. The coefficient of consolidation for bentonite is taken from Peppin et al. [24] (equivalent to their diffusivity), while the coefficient of consolidation for kaolinite is calculated using the same method as Peppin et al. [24] using fits to data from experiments on permeability and osmotic pressure [22, 25]. We are currently unaware of sufficient experimental data to calculate a value of the coefficient of consolidation for illite. Fracture toughness is that of Saint-Alban clay taken from Ayad et al[26]. The same estimate is used for each clay due to the lack of available data for separate clay types.

Constant	Bentonite	Illite	Kaolinite	Units
ν	0.3	0.3	0.3	-
k	5×10^{-20}	10^{-18}	10^{-17}	m^2
α	1	1	1	-
c	6.4×10^{-11}	-	5×10^{-8}	$\text{m}^2 \text{s}^{-1}$
K_{Ic}	1.5×10^3	1.5×10^3	1.5×10^3	$\text{Pa m}^{1/2}$

forming at a depth of 6-8cm in saturated Saint-Alban clay. This clay has the same characteristics as those of kaolinite in table 1 [26], and in the experiments was dried at an evaporation rate of $5 \times 10^{-8} \text{ m s}^{-1}$. It can be seen that this data point is also in good agreement with the predicted kaolinite spalling depth. Finally observations of drying in Death Valley, California (cf figure 1) show peel thicknesses of $O(2 \text{ mm})$ while the evaporation rate in this situation is estimated above to be $O(6 \times 10^{-7}) \text{ m s}^{-1}$. This point is included in figure 5 and although we are unable to determine the precise composition of the clay it can be seen that such cracking is very feasible for a typical mixture of clay types. An interesting result that can also be seen from the figure is that peels formed from higher permeability clays such as kaolinite under typical drying conditions are approximately 4cm thick and so are likely to be less common, being restricted to deeper soils, and also hard to observe due to fractures being deep and peels having minimal curvature.

Figure 6 shows the amount of time for a mud peel to occur as a function of the evaporation rate as calculated from equation (14). This figure shows that for typical warm evaporation rates ($E \approx 10^{-7} \text{ m s}^{-1}$), cracking will occur after approximately 20 minutes or more of drying, while for slower evaporation rates timescales can be on the order of 1-2 hours. This is in

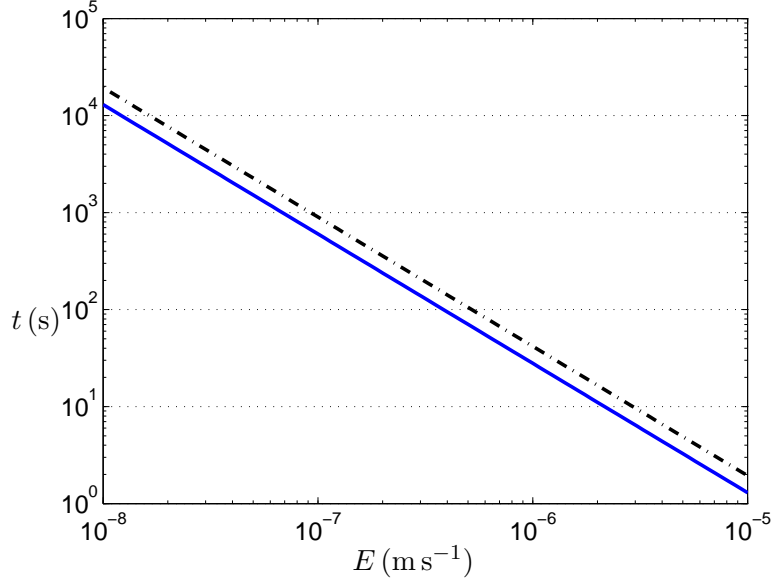


Figure 6: Time to fracture as a function of evaporation rate calculated for two types of clay. Continuous line: bentonite. Dash-dotted line: kaolinite.

agreement with the fact that peeling can occur in a tidal cycle [5] and so the timescale for cracking must be at most a few hours and in reality is expected to be substantially smaller.

We note that previous theories of mud peeling have attributed peel formation to the presence of stratification in the clay [5]. However these theories have been unable to explain the presence of multiple-layered peels as shown in figure 1. The new theory shows that mud peels can form in an isotropic layer of clay. Removal of old peels from the surface (by roll up due to the bending moment M in the peel) exposes the underlying clay which can then repeat the process of peel formation giving rise to multiple layers of peel. The increase in thickness in the underlying peels in figure 1 can also be explained by the fact that older peels will shield underlying clay which will lead to a lower evaporation rate E and hence thicker peels. Therefore the new theory appears to offer a qualitative and quantitative description of the phenomenon.

The theory also allows us to predict the curvature of the mud curls immediately after the horizontal fracture occurs. From plate theory, under plane strain conditions the radius of curvature of a plate subjected to a

moment per unit depth M is given by $R = E_y d^3 / 12M(1 - \nu^2)$ where E_y is Young's modulus. Then we can substitute equations (11) and (13) into this relationship to give the radius of curvature as a function of the peel thickness

$$R = 0.259 \frac{E_y d^{3/2}}{K_{Ic}(1 - \nu^2)}. \quad (15)$$

For a typical Young's modulus of $E_y = 5 \times 10^6$ Pa (e.g. [26]) this gives $R = 3.0$ cm for a 1 mm thick peel and $R = 0.95$ m for a 1 cm thick peel. These figures are in line with our expectations based on observations (e.g. figure (1) and the observations of Allen [5]). This equation should be of use as it is independent of evaporation rate, which can be difficult to measure in-situ in soils, and instead depends only on a small number of physical constants, Young's modulus E , Poisson's ratio ν and the fracture toughness K_{Ic} . The physical dimensions R and d should be much easier to measure in-situ and so we suggest that experimental verification of this relationship will serve as a simple test for our proposed theory. However, it should be noted that the relationship is only expected to hold directly after fracture occurs. Subsequent drying or desaturation of a curl will cause the stress distribution in the peel to alter along with its radius of curvature.

As a final comment on mud curl formation, we note that the fact that plasticity is occurring is illustrated by the mud curls in figure 1. If mud curls behaved poroelastically they should relax back to their initial, flat position upon desaturation. However the clay in the picture is fully dried and the peels are still curved indicating the presence of viscous or plastic behaviour during the process of peel formation and drying. This raises an interesting question as to how the curvature of the mud peels develops as the clay dries. In the case of a thicker (15mm deep), artificially-made mud curl, this has been explored theoretically and experimentally and it has been shown that the peels initially curl upwards before reducing or reversing their curvature upon desaturation [29, 30]. However in the case of thinner mud peels, the peels appear to remain tightly curled even after desaturation (c.f. figure 1). This is likely to be due to a combination of viscoplastic effects and the fact that the curvature of the peels are extreme enough to substantially modify the evaporation rates from their upper and lower sides. However there is insufficient experimental data at the current time to incorporate these effects into the model and we leave investigation of this effect to future work.

4.1 Analogy with thermoelastic spalling cracks

Although we have focused here on peel formation in a poroelastic solid, we note that the analysis can also be applied to the case of a thermoelastic solid being cooled from a surface with a fixed heat flux. In this case the temperature satisfies the diffusion equation (2) with c replaced by the thermal diffusivity κ . For a fixed heat flux Q at the surface,

$$Q = k_{th} \left. \frac{\partial T}{\partial z} \right|_{z=0} \quad (16)$$

where k_{th} is the thermal conductivity. Equation (5) is replaced with the appropriate expression for a thermoelastic solid,

$$\sigma_{xx} = \sigma_{yy} = \frac{\alpha_E E_y (T_0 - T)}{1 - \nu} \quad (17)$$

where α_E is the coefficient of thermal expansion, E_y is Young's modulus, T is temperature and T_0 is the reference temperature, and then we see that the two systems are equivalent up to a change in parameters. Thus the depth of spalling in a thermoelastic solid in the case of constant flux cooling can be obtained by a similar calculation to that presented here with appropriate parameter substitution.

5 Conclusions

In this paper we have demonstrated a new mechanism for the phenomenon of mud peeling in drying soils. Drying of a saturated soil leads to the presence of horizontal stresses due to reduction of pore pressure in the soil. We have analysed the system for the case of a constant evaporation rate E from the soil surface and shown that after a critical time a mode I crack can propagate parallel to the drying surface at a depth $d \sim E^{-2/3}$. Although there is currently little available data concerning mud peel thickness, we have calculated the spalling depth for typical clay permeabilities and shown that the results are in agreement with prior observations. The results also suggest that mud peeling is most likely to be observed in low permeability clays such as bentonite or illite. We hope this work will inspire systematic studies of the mud peeling phenomenon that can provide data for a rigorous testing of our results, and in anticipation we have suggested a convenient relationship between the thickness and radius of curvature of fresh mud peels that should serve as a simple experimental test of this theory.

Although we have focused on peeling of muds, our analysis is also applicable to delamination cracking in other deep layers of poroelastic solid undergoing a constant evaporation rate and in addition, due to the analogy between thermoelasticity and poroelasticity the results can be applied to the case of cooling of a thermoelastic solid by a simple exchange of parameters.

As well as explaining the physical mechanism that causes mud peeling, we note that just as shrinkage cracking is important in controlling the vertical permeability of soil to water and nutrients as well as other soil parameters, it is likely that peeling cracks are of a similar importance in controlling the horizontal permeability, a key parameter governing moisture and nutrient concentrations in soils. Our results should therefore be of use in predicting the formation of horizontal cracks and their effect upon soil characteristics during post-wetting desiccation and the subsequent period in which these cracks persist. This should be of interest in a diverse range of fields from plant sciences to the study of soil permeability in clay liners for hazardous waste containment.

6 Acknowledgments

This publication is based on work supported by Award No. KUK-C1-013-04, made by King Abdullah University of Science and Technology (KAUST).

References

- [1] S. Bohn, L. Pauchard, and Y. Couder. Hierarchical crack pattern as formed by successive domain divisions. i. temporal and geometrical hierarchy. *Phys. Rev. E*, 71:046214, 2005.
- [2] S. Bohn, J. Platkiewicz, B. Andreotti, M. Adda-Bedia, and Y. Couder. Hierarchical crack pattern as formed by successive domain divisions. ii. from disordered to deterministic behaviour. *Phys. Rev. E*, 71:046215, 2005.
- [3] J. E. Adams and R. J. Hanks. Evaporation from soil shrinkage cracks. *Soil Sci. Soc. Am. J.*, 28:281–284, 1964.
- [4] G. H. Omid, J. C. Thomas, and K. W. Brown. Effect of desiccation cracking on the hydraulic conductivity of a compacted clay liner. *Water, Air, Soil Pollut.*, 89:91–103, 1996.

- [5] J. R. L. Allen. On the curl of desiccation polygons. *Sedimentary Geology*, 46:23–31, 1986.
- [6] J. W. Hutchinson and Z. Suo. Mixed mode cracking in layered materials. *Adv. Appl. Mech.*, 29:63, 1992.
- [7] L. Goehring, L. Mahadevan, and S. W. Morris. Nonequilibrium scale selection mechanism for columnar jointing. *Proc. Natl. Acad. Sci. U. S. A.*, 106:387, 2009.
- [8] H. Peron, T. Hueckel, L. Laloui, and L. B. Hu. Fundamentals of desiccation cracking of fine-grained soils: experimental characterisation and mechanisms identification. *Can. Geotech. J.*, 46:1177–1201, 2009.
- [9] C. J. Martinez and J. A. Lewis. Shape evolution and stress development during latex-silica film formation. *Langmuir*, 18:4689–4698, 2002.
- [10] J. Graham and G. T. Houlsby. Anisotropic elasticity of a natural clay. *Geotechnique*, 33(2):165–180, 1983.
- [11] D. Muir Wood. *Soil behaviour and critical state soil mechanics*. Cambridge University Press, 1990.
- [12] P. H. Morris, J. Graham, and D. J. Williams. Cracking in drying soils. *Can. Geotech. J.*, 29:263–277, 1992.
- [13] H. F. Wang. *Theory of Linear Poroelasticity with Applications to Geomechanics and Hydrogeology*. Princeton University Press, 2000.
- [14] R. G. Robinson and M. M Allam. Effect of clay mineralogy on coefficient of consolidation. *Clays clay min.*, 46:596, 1998.
- [15] C. J. Brinker and G. W. Scherer. *Sol-Gel Science. The physics and chemistry of sol-gel processing*. Elsevier, 1990.
- [16] H. S. Carslaw and J. C. Jaeger. *Conduction of heat in solids*. Oxford University Press, 1959.
- [17] M. Abramovich and I. A. Stegun. *Handbook of Mathematical Functions*. Dover Publications, 1968.
- [18] J. R. Rice and M. P. Cleary. Some basic stress diffusion solutions for fluid-saturated elastic porous media with compressible constituents. *Rev. Geophys. Space Phys.*, 14(2):227–241, 1976.

- [19] M. D. Thouless, A. G. Evans, M. F. Ashby, and J. W. Hutchinson. The edge cracking and spalling of brittle plates. *Acta Met.*, 35:1333–1341, 1987.
- [20] J. Conaway and C. H. M. van Bavel. Evaporation from a wet soil surface calculated from radiometrically determined surface temperatures. *J. Appl. Meteor.*, 6:650–655, 1967.
- [21] H. K. A. Jassar, K. S. Rao, and I. Sabbah. A model for the retrieval and monitoring of soil moisture over desert area of kuwait. *Int. J. Rem. Sens.*, 27(2):329–348, 2006.
- [22] V. Pane and R. L. Schiffman. The permeability of clay suspensions. *Geotechnique*, 47:273–288, 1997.
- [23] S. S. L. Peppin, J. S. Wettlaufer, and M. G. Worster. Experimental verification of morphological instability in freezing aqueous colloidal suspensions. *Phys. Rev. Lett.*, 100:238301, 2008.
- [24] S. S. L. Peppin, A. Majumdar, and J. S. Wettlaufer. Morphological instability of an non-equilibrium ice-colloid interface. *Proc. Roy. Soc. A*, 466:177–194, 2010.
- [25] S. C. Brown and D. Payne. Frost action in clay soils. ii. ice and water location and suction of unfrozen water in clays below 0°C. *J. Soil. Sci.*, 41:547–561, 1990.
- [26] R. Ayad, J. M. Konrad, and M. Soulie. Desiccation of a sensitive clay: application of the model crack. *Can. Geotech. J.*, 34:943–951, 1997.
- [27] J. M. Konrad and R. Ayad. Desiccation of a sensitive clay: field experimental observations. *Can. Geotech. J.*, 34:929942, 1997.
- [28] J. R. L. Allen. Fine sediment and its sources, severn estuary and inner bristol channel, southwest britain. *Sed. Geol.*, 75:57–65, 1991.
- [29] G. Musielak and D. Mierzwa. Permanent strains in clay-like material during drying. *Drying Tech.*, 27:894–902, 2009.
- [30] G. W. Scherer. Drying gels iii. warping plate. *J. Non-Cryst. Solids*, 91(1):83–100, 1987.

RECENT REPORTS

20/10	Asymptotic expressions for the nearest and furthest dislocations in a pile-up against a grain boundary	Hall
21/10	Cardiac electromechanics: the effect of contraction model on the mathematical problem and accuracy of the numerical scheme	Pathmanathan Chapman Gavaghan Whiteley
22/10	Fat vs. thin threading approach on GPUs: application to stochastic simulation of chemical reactions	Klingbeil Erban Giles Maini
23/10	Asymptotic analysis of a system of algebraic equations arising in dislocation theory	Hall Chapman Ockendon
25/10	Preconditioning for Allen-Cahn Variational Inequalities with Non-Local Constraints	Blank Sarbu Stoll
26/10	On an evolution equation for sand dunes	Ellis Fowler
27/10	On Liquid Films on an Inclined Plate	Benilov Chapman McLoed Ockendon Zubkov
28/10	An a posteriori error analysis of a mixed finite element Galerkin approximation to second order linear parabolic problems	Memon Nataraj Pani
29/10	A Priori Error Estimates for Semidiscrete Finite Element Approximations to Equations of Motion Arising in Oldroyd Fluids of Order One	Goswami Pani
30/10	The Landau-de Gennes theory of nematic liquid crystals: Uniaxiality versus Biaxiality	Majumdar
31/10	The Radial-Hedgehog Solution in Landau-de Gennes' theory	Majumdar
32/10	Nonlinear instability in flagellar dynamics: a novel modulation mechanism in sperm migration?	Gadelha Gaffney Smith Kirkman-Brown
33/10	Error bounds on block GaussSeidel solutions of coupled multi-physics problem	Whiteley Gillow Tavener Walter
34/10	A random projection method for sharp phase boundaries in lattice Boltzmann simulations	Reis Dellar

35/10	Regularized Particle Filter with Langevin Resampling Step	Duan Farmer Moroz
36/10	Sequential Inverse Problems Bayesian Principles and the Logistic Map Example	Duan Farmer Moroz
37/10	Circumferential buckling instability of a growing cylindrical tube	Moulton Goriely
38/10	Preconditioners for state constrained optimal control problems with Moreau-Yosida penalty function	Stoll Wathen
39/10	Local synaptic signaling enhances the stochastic transport of motor-driven cargo in neurons	Newby Bressloff
40/10	Convection and Heat Transfer in Layered Sloping Warm-Water Aquifer	McKibbin Hale Style
41/10	Optimal Error Estimates of a Mixed Finite Element Method for Parabolic Integro-Differential Equations with Non Smooth Initial Data	Goswami Pani Yadav
42/10	On the Linear Stability of the Fifth-Order WENO Discretization	Motamed Macdonald Ruuth
43/10	Four Bugs on a Rectangle	Chapman Lottes Trefethen

Copies of these, and any other OCCAM reports can be obtained from:

**Oxford Centre for Collaborative Applied Mathematics
Mathematical Institute
24 - 29 St Giles'
Oxford
OX1 3LB
England
www.maths.ox.ac.uk/occam**